# Study on the quality change mechanism of Dioscorea alata during different storage periods based on transcriptome sequencing

**Peilong Wang**
Zhejiang Institute of subtropical crops
**Li Guan**
**Qiaoyi Zhang**
**Xinyue Li**
**Jiaqi He**
**Wan Xu**
**Zhimin Qiu**
**Gongkai Chen**
Wenzhou Vocational College of Science & Technol
**Zhuang Zhou**
zhuangchow@126.com

Zhejiang Institute of subtropical crops

**Research Article**

**Keywords:** Dioscorea alata, transcriptome analysis, starch, quality, storage

**Posted Date:** June 19th, 2026

**DOI:** https://doi.org/10.21203/rs.3.rs-9850474/v1



**Additional Declarations:** No competing interests reported.

# Study on the quality change mechanism of *Dioscorea alata* during different storage periods based on transcriptome sequencing

Peilong Wang[1,#], Li Guan[2,#], Qiaoyi Zhang[3], Xinyue Li[4], Jiaqi He[1], Wan Xu[1], Zhimin Qiu[1], Gongkai Chen[5,*], Zhuang Zhou[1,*]

[1] Zhejiang Institute of subtropical crops, Zhejiang academy of agricultural sciences, Wenzhou 325005, China

[2] School of Basic Medical, Jinzhou Medical University, Jinzhou, China

[3] Ecological Park Branch, Wenzhou Natural Resources and Planning Bureau, Wenzhou 325005, China

[4] Wenzhou Forestry Technology Promotion and Wildlife Protection Management Station, Wenzhou 325005, China

[5] Wenzhou Vocational College of Science & Technol, Wenzhou 325005, China

[#] These authors contributed equally to this work.

*** Correspondence:** zhuangchow@126.com, 447367668@qq.com.

## Abstract

*Dioscorea alata* is widely popular globally for its excellent medicinal and health-care properties, as well as delicious taste and good quality. However, *D. alata* easily browns during processing and storage, impairing quality and value, effective preservation is urgently needed. To explore the transcriptomic changes of *D. alata* during storage and provide a basis for its genetic research and quality improvement. HiSeq 2000 technology was used to sequence the transcriptomes of *D. alata* samples with different storage durations, and its key physiological indexes were determined. DEGs were identified in 10 d vs CK, 20 d vs CK, 30 d vs CK, and 40 d vs CK comparisons, with 1688, 2548, 6945, and 2185 DEGs respectively. A total of 666 common DEGs were found across all four groups; functional annotation showed they might be involved in molecular functions, cellular components and biological processes. Genes related to starch and sucrose metabolism, as well as TFs in DEGs, were analyzed systematically. The transcriptomic data and analysis provide valuable insights for future *D. alata* gene exploration, molecular marker development and quality improvement.

**Keywords** *Dioscorea alata*, transcriptome analysis, starch, quality, storage.

## Introduction

*Dioscorea alata* L. is an annual or perennial twining vine with dicotyledonous characteristics (Jing et al. 2016). Yam is rich in starch, fiber, polysaccharide, saponin, dioscin, allantoin, flavonoids and polyphenols, which have pharmacological effects such as invigorating the spleen and stomach and enhancing immunity. Its unique flavor and function make its processed products have good market prospects (Li et al. 2023). However, during the processing and storage of yam, it often produces intense browning and loses its original milky white color, which seriously affects the appearance, flavor and commodity value of the product (Gu et al. 2006). Moreover, yam is prone to quality deterioration problems such as yellowing, browning, softening, deterioration, nutrient loss and rot during storage. Some varieties of yam are too big for consumers to eat completely at one time. The cut yam is prone to quality degradation and pollution, which not only affects the nutritional value of yam, but also reduces the acceptance of consumers (Gündüz et al. 2019). Therefore, how to effectively process and store yam to ensure its quality and taste has become an urgent problem (He et al. 2024).

In recent years, to delay the browning and quality deterioration of yam, chemical, physical, and comprehensive treatments have been commonly employed. The changes of eight indexes of fresh-cut yam during 14 days of storage under five different shelf temperatures analyze results indicated that a low temperature of 1℃ was most conducive to maintaining quality, with the yam retaining good appearance even after 14 days of storage. In contrast, at room temperature (20℃), the yam lost its edibility after 7 days. Samples without exogenous bacteriostatic treatment exhibited a high total colony count that increased rapidly, and the activities of PPO and POD were more than 10 times those of PAL (Gao et al. 2022). Liao et al. found that fresh-cut *D. alata* stored at -18℃ maintained the best comprehensive quality, whether stored for a short term of 10 days or a long term of 100 days (Liao et al. 2021). Ma et al. demonstrated that ice-temperature storage could effectively delay the browning of fresh-cut yam, reduce the weight loss rate and MDA content, maintain PPO activity at an appropriate level, and keep microbial counts low, thereby better preserving the quality of fresh-cut yam (Ma et al. 2021). Wu et al. found that under the same processing conditions, storage time had no significant effect on the quality of purple yam but exerted a significant influence on the other two varieties. Specifically, the weight loss rate showed a significant difference in the late storage period, while no significant differences were observed in protein and fat contents (Wu et al. 2025). The low-concentration EA treatments could effectively maintain CAT activity and reduce the accumulation of total phenols, thereby significantly inhibiting pulp browning (Li et al. 2024). Liu et al. reported that fresh-cut yam treatments with 0.08% $NaHSO_3$ and 25% ethanol solution could significantly reduce the browning degree, inhibit the activities of PPO, respiration rate, and microbial growth, thus better maintaining the commercial value of it (Liu et al. 2015). Meng et al. found that sodium hypochlorite exhibited the best sterilization effect on fresh-cut yam. Soaking in a solution of 1.0% citric acid + 0.5% calcium chloride for 10 minutes achieved the optimal color protection effect, while fumigation with 200 μL/L ethanol for 3 hours showed the best performance in controlling microorganisms and inhibiting browning (Meng et al. 2020). Ma et al. discovered that coating fresh-cut yam with a composite film consisting of 1.57% chitosan, 0.9% carrageenan, and 1.55% sodium alginate could significantly reduce the browning degree and PPO specific activity during storage. Furthermore, this coating could prevent the oxidation of phenols in the late storage period, thereby enhancing the overall antioxidant capacity of fresh-cut yam (Ma et al. 2012). Studies identified that 0.6% onion oil + 1.0% citric acid + 1.0% chitosan as the optimal preservative can inhibits PPO and POD activities, reduces relative conductivity and MDA content, delays quality deterioration, and extends the shelf life by about 6 days (Wang et al. 2017). Yang et al. reported that immersion of yam in a composite solution consisting of 0.6% salt, 0.4% sucrose and 0.4% acetic acid for 15 min, followed by packaging with PP/PE film, exhibited the optimal preservation efficacy (Yang et al. 2018).

*D. alata* is highly favored by the market due to its high nutritional value, excellent taste, high economic value, and great processing potential, thus attracting increasing attention from breeding experts. Wencheng *D. alata*, as an excellent local variety, has become a new favorite in the market owing to its unique taste and medicinal value. With its expanding market influence, it has also gained great attention from the local government. However, the current research on Wencheng *D. alata* is still in its initial stage. Specifically, there are few studies on the storage of *D. alata*, limited reports on its storage quality, and no technical means to accurately regulate the starch content and composition for *D. alata* storage. These issues have seriously hindered the further

development of the Wencheng *D. alata* industry.

For species lacking genome information, transcriptome sequencing can generate a large volume of data, which is conducive to mining important functional genes and serves as a crucial approach for conducting research on excellent plant traits (Gebeyehu et al. 2019; Zheng et al. 2026; Deng et al. 2026). With the continuous advancement of high-throughput sequencing technology, sequencing costs have decreased significantly, while abundant sequencing data can be obtained. This not only facilitates transcriptome analysis, gene structure and function research, but also lays a foundation for the development of numerous molecular markers (Fang et al. 2014; Feng et al. 2014). In view of this, the present study employed DNBSEQ platform sequencing technology to perform transcriptome sequencing and analysis on *D. alata*. A large amount of sequencing data was obtained, spliced and assembled to establish the transcriptome database of *D. alata*. Combined with bioinformatics methods, functional annotation, functional classification and metabolic pathway analysis were conducted on the sequences in the transcriptome database. This study aims to lay a foundation for genome-level research on *D. alata*, and also provide theoretical ideas for the storage of *D. alata* and the development of high-quality products.

## Materials and methods

### Plant materials and indicators determination

The experimental materials were cultivated in the Resource Garden of Zhejiang Institute of Subtropical Crops. Harvested *D. alata* tubers were stored for 10 d, 20 d, 30 d, and 40 d, respectively, with freshly collected samples served as the control (CK). Starch content was determined via anthrone colorimetry using a biochemical kit (Norminkoda Biotechnology Co., Ltd. Wuhan,China). Amylose content in the samples were measured by iodine-binding colorimetry, with absorbance recorded at 620 nm. Moisture content was analyzed following the standard method described by Chen et al (Chen et al. 2014). The fresh weight of the homogenate was weighed first, then the homogenate was dried in an oven at 70 ℃ to a constant weight, and moisture content was calculated accordingly. Crude protein content in the samples was detected by the Kjeldahl method (Wassie et al. 2025), while crude fat content was determined using Soxhlet extraction (GB 5009.6-2025). Ascorbic acid (ASA) content was assayed by colorimetry (Li et al. 2023). For vitamin E (VE) content determination, colorimetry was also adopted based on the characteristic that VE reduces $Fe^{3+}$ to $Fe^{2+}$, the generated $Fe^{2+}$ forms a colored complex with 1,10-phenanthroline, which has a characteristic absorption peak at 530 nm, and VE content was calculated by measuring the absorbance at this wavelength (Kim et al. 2025). The α-amino group of amino acids can react with hydrated ninhydrin to form a blue-purple compound with a characteristic absorption peak at 570 nm. Amino acid content in the samples was thus calculated by determining the absorbance at 570 nm (Tang et al. 2026). Total polysaccharides were extracted by water extraction and alcohol precipitation, and their content was quantified by the phenol-sulfuric acid method (Phosarith et al. 2025). Meanwhile, pearson correlation analysis was performed to explore the correlations among the contents of various indicators in the samples.

### RNA extraction, library construction, sequencing, and de novo assembly

Total RNA was extracted from the collected materials using the CTAB method (Jiang et al. 2003). The quality and quantity of total RNA were identified and quantified by a Qubit fluorometer and a Qsep400 high-throughput biological fragment analyzer, respectively.

Subsequently, equal amounts of high-quality RNA from each sample were used for DNA library construction, and sequencing was performed on the Illumina HiSeq 2000 platform (Illumina Inc. CA, USA). After transcriptome sequencing, the quantity and length of raw data were counted. Clean reads were obtained by removing sequencing adapters, redundant sequences, and low-quality reads from the raw data. Specifically, reads with more than 10% unknown bases, adapters, and low quality were filtered out from each dataset. High-quality clean reads were then assembled using Trinity software, and the resulting transcript sequences were used as reference sequences for subsequent analyses (Grabherr et al. 2011).

**Sequence annotation, functional classification, and biological pathway analysis**

Bioinformatics analysis was performed on the obtained unigenes, including functional annotation and classification. The spliced unigene sequences were aligned against protein databases using BLAST, with annotations acquired at a threshold of e-value < 0.00001, covering the NR and Swiss-Prot databases. E-value, similarity, and species distribution were analyzed by alignment with the NR database. Based on the annotation information from NR, Gene Ontology (GO) annotations were obtained using Blast2GO software (Conesa et al. 2005). GO consists of three relatively independent categories: Biological Process, Cellular Component, and Molecular Function. All unigenes were classified using WEGO to macroscopically understand the distribution characteristics of gene functions in *D. alata* (Ye et al. 2006). Unigenes were also aligned against the COG database for functional classification and statistical analysis of their potential functions (Tatusov et al. 2000). Meanwhile, Kyoto Encyclopedia of Genes and Genomes (KEGG) metabolic pathway analysis was conducted to further elucidate the metabolic pathways, biological functions, and gene interactions in *D. alata* (Kanehisa et al. 2004). In addition, TransDecoder software was used to identify candidate coding regions in unigenes: first, the longest open reading frame (ORF) was extracted, followed by searching for homologous sequences of Pfam proteins through BLAST alignment against the SwissProt database and Hmmscan, thereby predicting the coding regions.

**Analysis of differentially expressed genes (DEGs)**

To investigate transcriptional changes in *D. alata* during different storage periods, DEGs in samples stored for 10 d, 20 d, 30 d, and 40 d were identified by comparing their expression levels with those of CK. The false discovery rate (FDR) was calculated to adjust the p-value threshold, thereby correcting for multiple testing (Rajkumar et al. 2015). Unigenes meeting the screening criteria of $|\log2Ratio| \geq 1$ and FDR $\leq 0.001$ were considered differentially expressed between groups. DEGs with higher expression levels than CK at 10 d, 20 d, 30 d, and 40 d were defined as "up-regulated," while those with lower expression levels were designated as "down-regulated." Venny 2.0 (https://bioinfogp.cnb.csic.es/tools/venny/index 2.0.2.html) was used to generate a Venn diagram of DEGs to visualize group-specific and overlapping differences. Subsequently, STEM 1.3.8 software was applied to analyze DEG expression patterns (Ernst et al. 2006). When the p-value was < 0.05, DEGs with similar expression patterns were clustered into the same category using K-means clustering.

**Transcription factor (TF) statistics and data analysis**

iTAK software was used to analyze unigenes in the transcriptome data, and the types and

quantities of all transcription factors (TFs) as well as TFs among DEGs were statistically summarized (Zheng et al. 2016). Additionally, a heatmap was constructed for the major TFs in DEGs to analyze their expression trends. Based on the RNA-Seq expression data, 12 significantly differentially expressed transcription factor genes, belonging to the bHLH, MYB, WRKY, NAC, ERF, and C2H2 families, were selected for qRT-PCR validation. Specific primers for the 12 candidate genes and the internal reference gene CKI2 were designed using the NCBI Primer-BLAST tool, with primer lengths of 18–25 bp, amplicon lengths of 80–200 bp, and melting temperature (Tm) values of 58–62 ℃. All primer sequences were synthesized by Sangon Biotech (Shanghai) Co., Ltd. First-strand cDNA was synthesized from total RNA of each time point using the HiScript III RT SuperMix reverse transcription kit. qRT-PCR was performed on a Archimed X4 instrument (Kunpeng Gene (Beijing) Scientific Instrument Co., Ltd.) using the SYBR Green fluorescent dye method. The 20 μL reaction mixture contained 10 μL of 2×SYBR qPCR Master Mix, 1.0 μL of each forward and reverse primer (10 μmol/L), 2 μL of cDNA template, and 6.0 μL of $ddH_2O$. The thermal cycling protocol was as follows: pre-denaturation at 95 ℃ for 30 s; 40 cycles of denaturation at 95 ℃ for 10 s and annealing/extension at 60 ℃ for 30 s; followed by melting curve analysis (95 ℃ for 15 s, 60 ℃ for 1 min, 95 ℃ for 15 s) to confirm amplification specificity. Relative expression levels of target genes were calculated using the $2^{-\Delta\Delta Ct}$ method, normalized to the CKI2 reference gene and using the CK group as the calibrator. RNA-Seq data were presented as FPKM values to represent gene expression levels. The consistency of expression trends detected by the two techniques was analyzed to validate the reliability of the transcriptomic sequencing data.

## Results

### Physiological indexes analysis of *D. alata* under different storage durations

The related physiological indexes of *D. alata* exhibited distinct variation trends with different storage durations. During the entire storage period, the water content of *D. alata* showed a gradual decreasing trend. For total polysaccharide content, it decreased in the early storage stage (10–20 days), increased sharply around the 30 day, and then decreased slightly after 40 days of storage. With the extension of storage time, both starch and amylopectin contents continued to decrease. The VE content changed relatively gently in the early stage (10–20 days), but increased significantly in the late storage stage (30–40 days). The VC content remained at a low level with little fluctuation in the early stage (10–20 days), increased sharply around 30 days, and decreased again at 40 days of storage. As for amino acid content, it decreased first and then increased with prolonged storage, with a significant increase observed after approximately 30 days of storage. Similarly, the crude protein content showed a trend of first decreasing and then increasing, with a significant increase during the 30–40 day storage period. In contrast, the crude fat content increased significantly in the late storage stage (30–40 days) (Fig. 1).

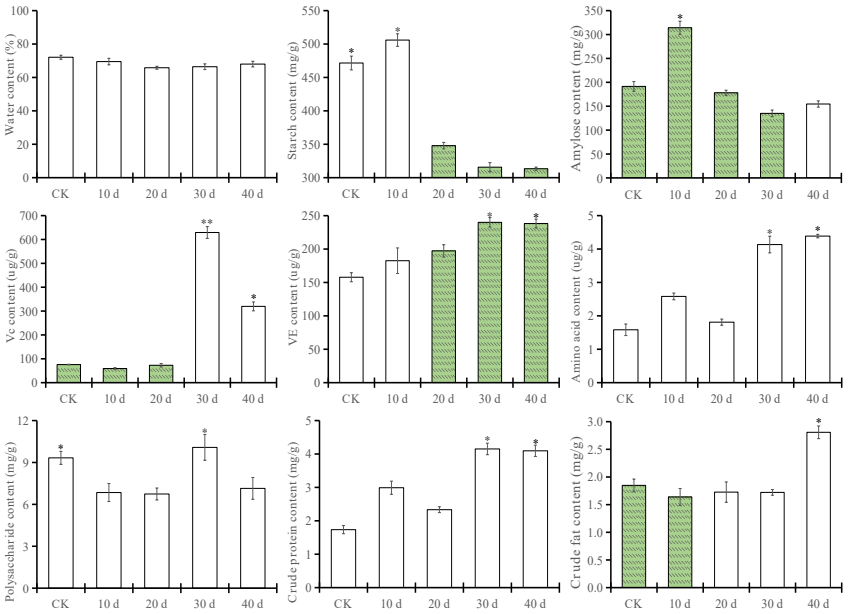


**Fig. 1. Analysis of related physiological indexes of *D. alata* under different storage durations.** Note: "*" indicates significant differences ($p < 0.05$).

Correlation analysis of the above indexes revealed that starch content (including total starch and amylopectin) decreased with the extension of storage time, which was consistent with the gradual decrease in water content, indicating a positive correlation between them. The crude protein content and amino acid content showed similar variation characteristics of "first decreasing and then increasing", presenting a positive correlation trend. As important vitamins, VE and VC may have a negative correlation with nutrient decomposition indexes. Their increased contents in the late storage stage might be positively correlated with the transformation indexes of related substances. Additionally, the crude fat content was found to be negatively correlated with starch content (Fig. 2).

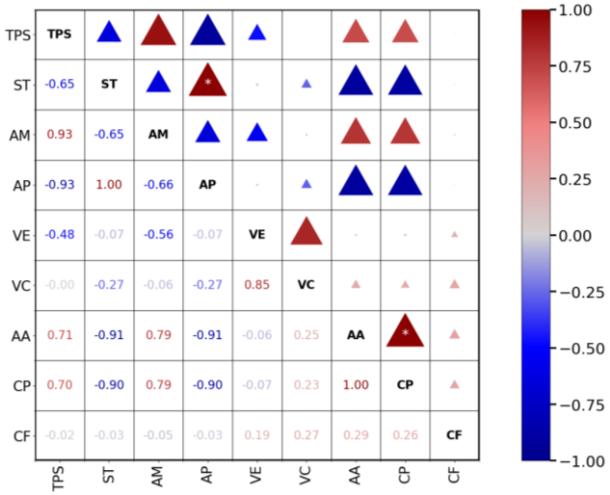


**Fig. 2. Correlation analysis of related physiological indexes of *D. alata* under different storage durations.**

## Transcriptome sequencing and de novo assembly of *D. alata* under different storage durations

Given the significant differences in the content of related physiological indexes of *D. alata* under different storage durations, which are closely associated with its variety quality, samples at different storage time points (CK, 10 d, 20 d, 30 d, and 40 d) were subsequently selected for transcriptome RNA-seq analysis. Total RNA was extracted from the five samples, followed by sequencing using the Illumina HiSeq Xten platform. A total of 17.40 Gb of clean data was obtained in this project, with each sample yielding more than 3.34 Gb of clean data and the Q30 percentage exceeding 93% (Table 1).

Table 1. Summary of generated RNA-seq data.

| NO | Raw Reads (M) | Q30（%） | GC（%） | Clean Reads | Total Mapping（%） | Uniquely Mapping（%） |
|---|---|---|---|---|---|---|
| CK | 47.08 | 94.13 | 46.55 | 47125060 | 93.42 | 89.94 |
| 10 d | 45.91 | 93.53 | 46.5 | 45824826 | 93.24 | 90.10 |
| 20 d | 48.27 | 94.03 | 46.38 | 48887186 | 92.72 | 89.73 |
| 30 d | 53.78 | 93.94 | 42.6 | 38661872 | 82.41 | 80.24 |
| 40 d | 46.49 | 93.46 | 46.33 | 46799572 | 92.53 | 89.02 |

**Analysis and identification of DEGs in *D. alata* under different storage durations**

Comprehensive analysis of DEGs at 10d, 20d, 30d, and 40d relative to CK revealed dynamic expression patterns over time. MA plots showed that the distribution of upregulated (red) and downregulated (blue) genes was most dispersed at 30d (Fig. 3A), indicating the largest amplitude of gene expression perturbation at this time point. Volcano plots quantified that the total number of significant DEGs peaked at 30d, markedly exceeding those at 10d, 20d, and 40d (Fig. 3B). Radar plots further visualized that the $\log_2$FC of DEGs at 30d spanned the widest range, with both upregulation and downregulation magnitudes notably greater than those at other time points, while the 10d group exhibited the smallest differential amplitude (Fig. 3C). Unigenes with a q-value < 0.05 and $|\log_2 FC| \geq 1$ were defined as DEGs. Compared with CK, 1688, 2548, 6945, and 2185 DEGs were identified in the samples stored for 10 d, 20 d, 30 d, and 40 d, respectively. Specifically, the number of up-regulated genes in these four storage groups was 1040, 1579, 3618, and 1246, respectively, while the number of down-regulated genes was 648, 969, 3327, and 939, respectively (Fig. 3D). The number of DEGs showed an increasing trend among the four experimental groups, with the 30 d vs CK group exhibiting the highest number of DEGs. To further clarify the DEGs among *D. alata* samples with different storage durations, a Venn diagram was constructed to analyze the overlap of DEGs between the 10 d vs CK, 20 d vs CK, 30 d vs CK, and 40 d vs CK groups. The results showed that 666 DEGs were commonly shared among the four groups (Fig. 3E).

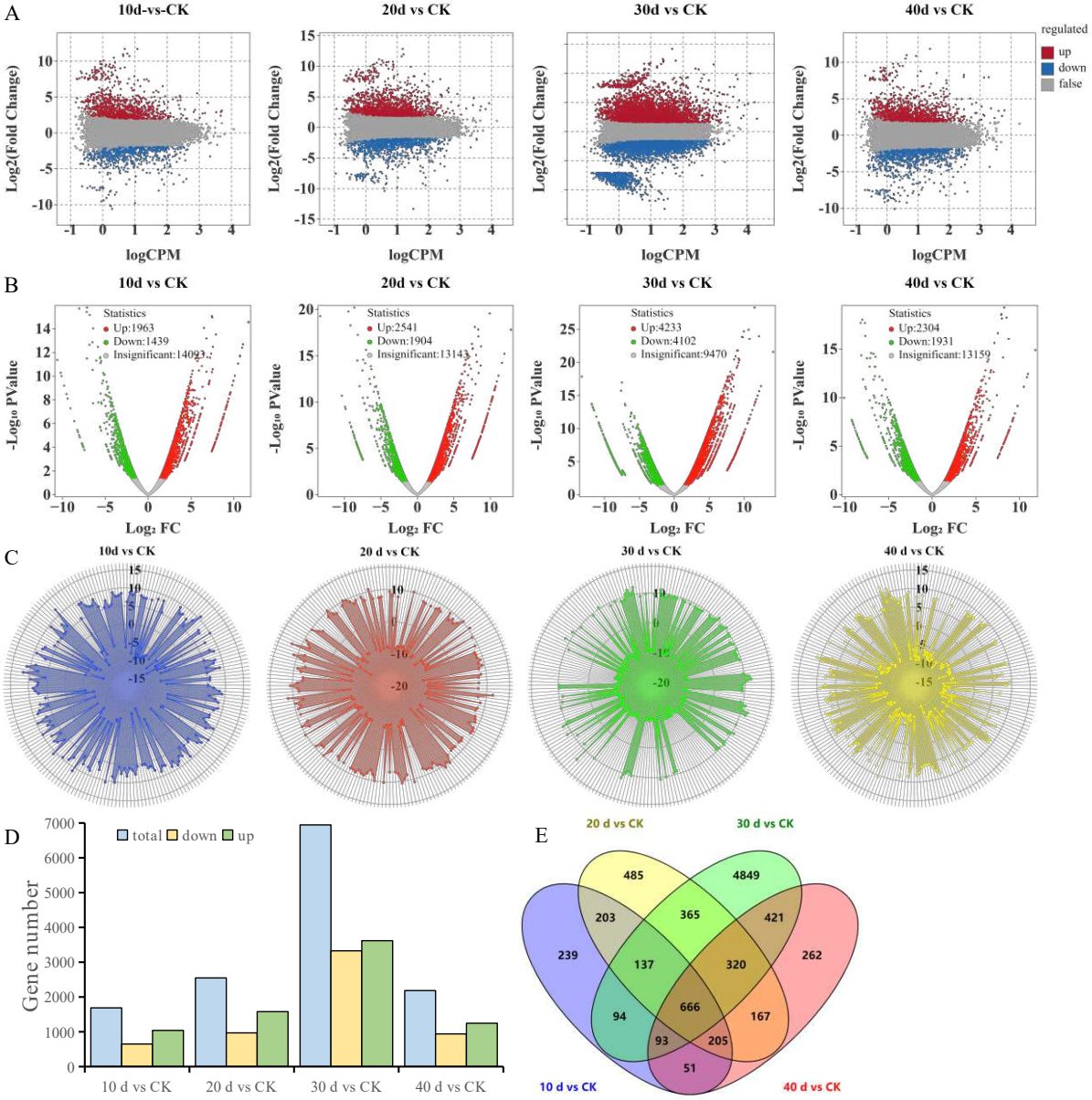


**Fig. 3. Expression patterns of DEGs in *D. alata* under different storage durations.** (A) MA plot, (B) Volcano plot and (C) Radar chart between the 10 d vs CK, 20 d vs CK, 30 d vs CK, and 40 d vs CK groups. (D) Quantitative statistics of DEGs. (E) Venn diagram of DEGs.

To clarify the functions of DEGs, enrichment analyses of GO and KEGG pathways were performed. GO annotation results showed that DEGs in *D. alata* samples under different storage durations were significantly enriched in biological processes and molecular functions related to metabolic processes and catalytic activities (Fig. 4A, B). Specifically, DEGs associated with biological processes, cellular processes, and metabolic processes were enriched at all four treatment time points, in most cases, the number of DEGs in these categories gradually increased across the four time points, reaching a peak at 30 d (Fig. 4A). In terms of molecular functions, DEGs with binding and catalytic activities exhibited relatively high abundance, and their numbers also showed a gradual increasing trend across the four treatment time points, peaking at 30 d (Fig. 4B). These results suggest that these genes or their encoded proteins are involved in cellular metabolic processes and play important roles in the storage of *D. alata*.

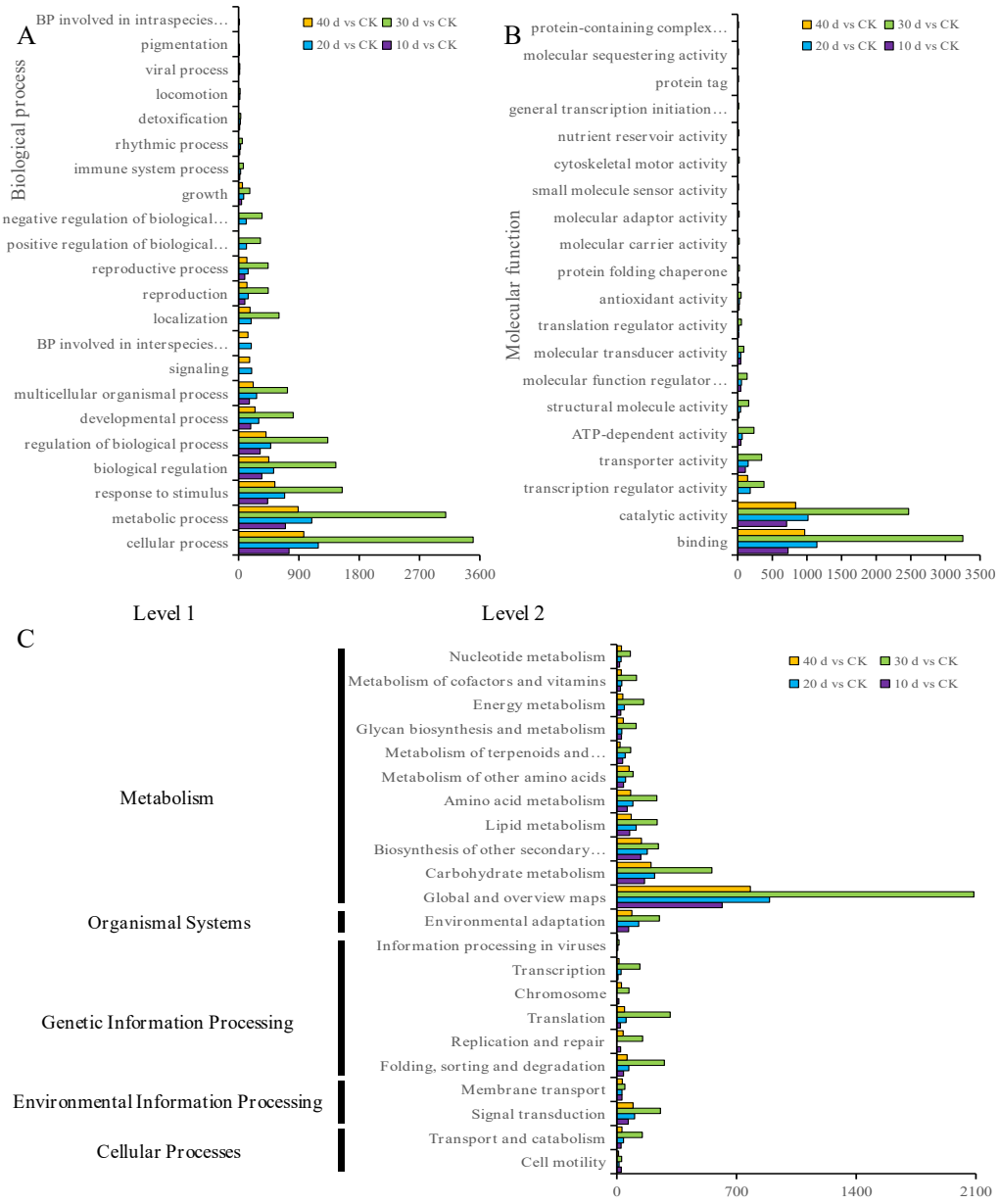


**Fig. 4. GO terms and KEGG pathways analysis of DEGs.** Statistical analysis of DEGs in biological process terms (A), molecular function terms (B) from GO annotation, and KEGG pathways (C) in *D. alata* under different storage durations. The x-axis in (A, B) represents the number of DEGs in each GO term, while the x-axis in (C) represents the number of DEGs in each KEGG pathway.

KEGG pathway enrichment analysis results showed that paired comparisons (10 d vs CK, 20 d vs CK, 30 d vs CK, and 40 d vs CK) identified 127, 130, 144, and 130 pathways, respectively. These pathways included 22 secondary pathways and 5 primary pathways. Based on these findings, DEGs were highly enriched in "Global and Overview Diagram, Carbohydrate Metabolism, and Translation" (Fig. 4C). Meanwhile, we observed that among the top 30 pathways in the 10 d vs CK comparison, 8 were related to carbon metabolism, and 6 carbon metabolism-related pathways were found among the top 20 pathways (Table 2). These results indicate that the genes involved in carbon metabolism may play crucial roles in sugar transformation of *D. alata* during storage.

Table 2. Top 30 KEGG pathways based on the percentage of DEGs in the 10 d vs CK comparison.

| Term | 10 d vs CK | | 20 d vs CK | | 30 d vs CK | | 40 d vs CK | |
|---|---|---|---|---|---|---|---|---|
| | DEGs | % | DEGs | % | DEGs | % | DEGs | % |
| Metabolic pathways | 322 | 21.02 | 453 | 20.13 | 1061 | 18.66 | 403 | 20.72 |
| Biosynthesis of secondary metabolites | 221 | 14.43 | 315 | 14.00 | 601 | 10.57 | 264 | 13.57 |
| Plant-pathogen interaction | 52 | 3.39 | 114 | 5.07 | 207 | 3.64 | 68 | 3.50 |
| Phenylpropanoid biosynthesis | 39 | 2.55 | 54 | 2.40 | 57 | 1.00 | 33 | 1.70 |
| Starch and sucrose metabolism | 34 | 2.22 | 50 | 2.36 | 93 | 1.64 | 36 | 1.85 |
| Plant hormone signal transduction | 34 | 2.22 | 53 | 2.40 | 139 | 2.45 | 52 | 2.67 |
| ABC transporters | 30 | 1.96 | 30 | 1.51 | 47 | 0.83 | 32 | 1.65 |
| Flavonoid biosynthesis | 27 | 1.76 | 29 | 1.33 | 33 | 0.58 | 25 | 1.29 |
| MAPK signaling pathway - plant | 27 | 1.76 | 40 | 2.22 | 89 | 1.57 | 35 | 1.80 |
| Motor proteins | 26 | 1.70 | 13 | 0.00 | 28 | 0.49 | 10 | 0.51 |
| Glycerolipid metabolism | 23 | 1.50 | 22 | 1.07 | 37 | 0.65 | 24 | 1.23 |
| Glycolysis / Gluconeogenesis | 19 | 1.24 | 24 | 1.11 | 57 | 1.00 | 27 | 1.39 |
| Pentose and glucuronate interconversions | 19 | 1.24 | 21 | 0.98 | 36 | 0.63 | 20 | 1.03 |
| Biosynthesis of cofactors | 19 | 1.24 | 24 | 1.07 | 93 | 1.64 | 20 | 1.03 |
| Carbon metabolism | 18 | 1.17 | 34 | 1.51 | 115 | 2.02 | 35 | 1.80 |
| Circadian rhythm - plant | 17 | 1.11 | 14 | 0.62 | 42 | 0.74 | 20 | 1.03 |
| Glutathione metabolism | 16 | 1.04 | 18 | 0.84 | 37 | 0.65 | 24 | 1.23 |
| Biosynthesis of various plant secondary metabolites | 16 | 1.04 | 19 | 0.93 | 33 | 0.58 | 20 | 1.03 |
| Galactose metabolism | 16 | 1.04 | 18 | 0.80 | 41 | 0.72 | 18 | 0.93 |
| Amino sugar and nucleotide sugar metabolism | 16 | 1.04 | 28 | 1.29 | 72 | 1.27 | 22 | 1.13 |
| Biosynthesis of amino acids | 16 | 1.04 | 27 | 1.24 | 93 | 1.64 | 25 | 1.29 |
| Zeatin biosynthesis | 15 | 0.98 | 15 | 0.00 | 18 | 0.32 | 12 | 0.62 |
| Isoflavonoid biosynthesis | 14 | 0.91 | 13 | 0.62 | 36 | 0.63 | 18 | 0.93 |
| Fructose and mannose metabolism | 13 | 0.85 | 18 | 0.80 | 37 | 0.65 | 16 | 0.82 |
| RNA degradation | 13 | 0.85 | 14 | 0.62 | 55 | 0.97 | 11 | 0.57 |
| Cyanoamino acid metabolism | 12 | 0.78 | 16 | 0.71 | 25 | 0.44 | 14 | 0.72 |
| Protein processing in endoplasmic reticulum | 12 | 0.78 | 34 | 1.78 | 107 | 1.88 | 23 | 1.18 |
| Other glycan degradation | 11 | 0.72 | 11 | 0.49 | 24 | 0.42 | 14 | 0.72 |
| Ubiquinone and other terpenoid-quinone biosynthesis | 11 | 0.72 | 16 | 0.00 | 21 | 0.37 | 9 | 0.46 |
| Tropane, piperidine and pyridine alkaloid biosynthesis | 11 | 0.72 | 12 | 0.53 | 15 | 0.26 | 9 | 0.46 |

277 KEGG pathway related to carbon metabolism has a gray background

278 **Analysis of expression pattern of DEGs**

279 DEGs was systematically clustered, and the results showed that DEGs with similar
280 expression trends were assigned to six different groups. including 2010, 488, 936, 781, 2729 and
281 1613 genes respectively, in which C1 and C6 groups mainly showed down-regulation trend, while
282 C4 and C5 groups mainly showed up-regulation trend (Fig. 5).

283 The expression level in the C1 group exhibited a declining trend, hitting the minimum at 30 d
284 and then rising slightly at 40 d. In the C2 group, the expression level increased initially, peaked at
285 10 d, and subsequently declined. The C3 group showed an increase in expression level over the
286 first two stages, which peaked at 20 d and then decreased. Expression in the C4 group rose
287 continuously across all stages, reaching its maximum at 40 d. For the C5 group, the expression

level increased over the first three stages, peaked at 30 d, and then declined thereafter. In the C6 group, the expression level decreased over the first three stages, fell to the minimum at 30 d, and then increased.

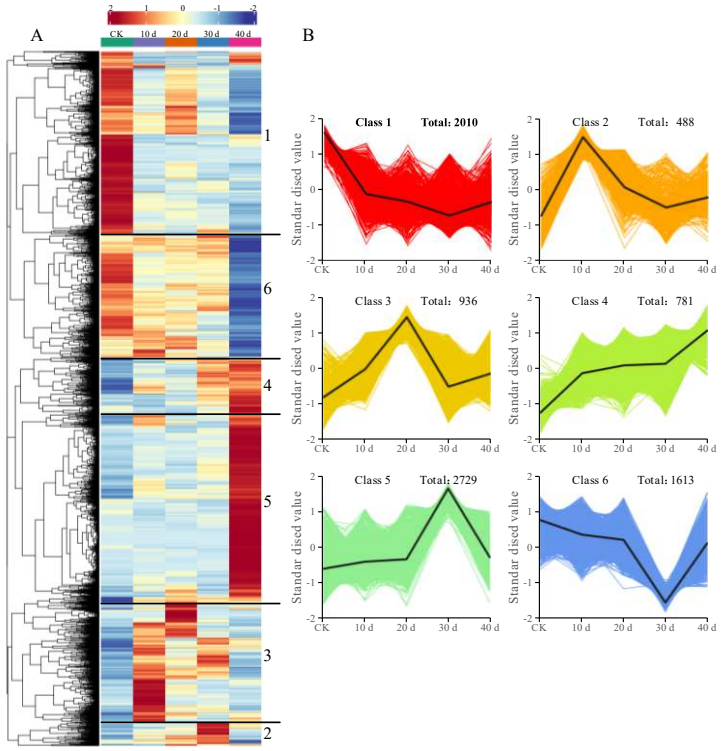


**Fig. 5. Temporal expression pattern analysis of all DEGs.** (A) Heatmap analysis of DEGs. (B) Expression trend pattern analysis of DEGs.

Based on the significant clustering results of KEGG pathway analysis, DEGs in the C4 and C5 groups exhibited an upward expression trend, whereas those in the C1 and C6 groups showed a downward trend (Fig. 5). Additionally, pathway enrichment analysis of DEGs in these four groups revealed that they were mainly involved in metabolic pathways, biosynthesis of secondary metabolites, hormone signal transduction, and plant-pathogen interaction (Fig. 6), suggesting that these pathways play crucial roles in the storage of *D. alata* at different time points. Thus, DEGs associated with these pathways were further analyzed. Through GO functional annotation analysis, the number of DEGs in each group was counted according to three categories: biological process (BP), molecular function (MF), and cellular component (CC). The results indicated that 541 out of 666 DEGs were annotated to 2677 functional pathways. Among these, DEGs involved in molecular function, cellular component, cellular anatomical entity, and biological process accounted for relatively large proportions, with 467, 440, 437, and 408 genes, respectively (Table 3).

Collectively, the results of K-means/phylogenetic clustering and GO functional annotation demonstrated that genes related to carbon metabolism were significantly affected during the different storage periods of *D. alata*. Therefore, DEGs associated with these pathways were further subjected to systematic analysis.

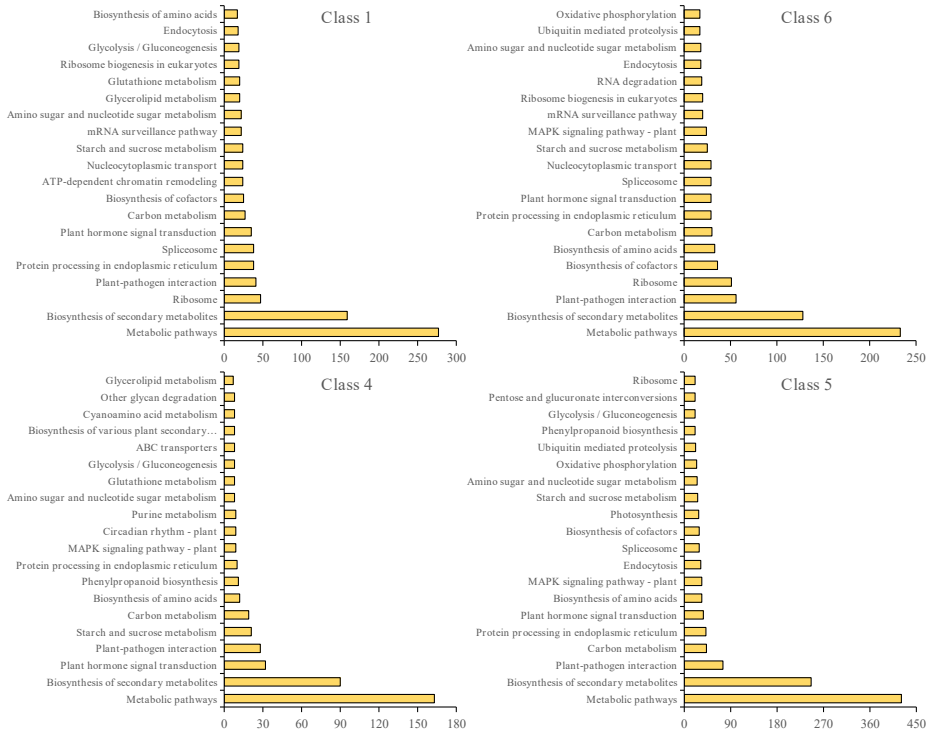


**Fig. 6. KEGG analysis of significant clusters ($p < 0.05$) in *D. alata*.**

Table 3. The top 20 GO function based on number of common DEGs.

| Gene Ontology Molecular Function | DEG_item |
|---|---|
| molecular_function | 467 |
| cellular_component | 440 |
| cellular anatomical entity | 437 |
| biological_process | 408 |
| binding | 295 |
| catalytic activity | 294 |
| cellular process | 293 |
| metabolic process | 289 |
| intracellular anatomical structure | 281 |
| organic substance metabolic process | 265 |
| organelle | 237 |
| intracellular organelle | 235 |
| membrane-bounded organelle | 233 |
| intracellular membrane-bounded organelle | 228 |
| primary metabolic process | 209 |
| cellular metabolic process | 207 |
| organic cyclic compound binding | 199 |
| heterocyclic compound binding | 198 |
| ion binding | 187 |
| membrane | 183 |

## DEG expression profile of starch and sucrose metabolism in *D. alata* under different storage durations

Based on STEM analysis and KEGG annotation results, a total of 14 DEGs related to starch and sucrose metabolism were identified in *D. alata* under different storage durations. These 14 DEGs were mainly involved in five metabolic pathways (Fig. 7). Among the 14 DEGs, twelve mainly exhibited an up-regulation trend. Specifically, six of these up-regulated genes encoded endoglucanase and were involved in the metabolic process of converting cellulose to cellodextrin, three genes encoded β-glucosidase and participated in the metabolic process of converting cellodextrin to cellobiose; and another three genes encoded α-amylase, which was involved in catalyzing the conversion of starch and glycogen to dextrin. In addition, the remaining two DEGs mainly showed a down-regulation trend. One of these down-regulated genes encoded trehalose-6-phosphate phosphatase and participated in the catalytic process of converting trehalose-6-phosphate to D-glucose-6-phosphate, the other gene encoded endoglucanase/1,3-β-glucosidase and was involved in catalyzing the conversion of 1,3-β-glucan to D-glucose.

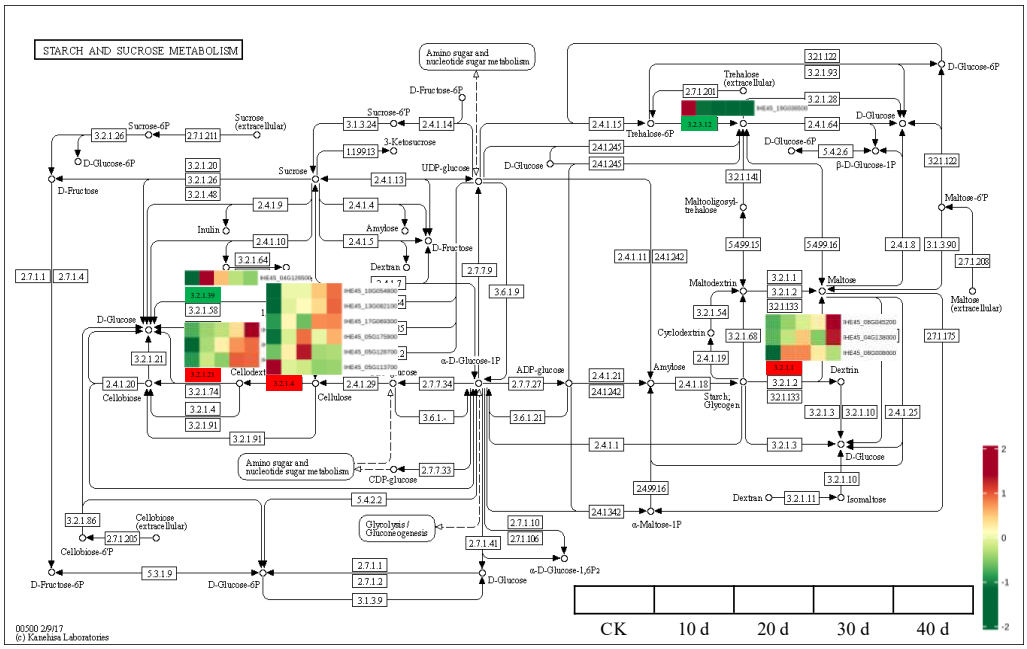


**Fig. 7. Metabolic pathways involved in starch and sucrose metabolism-related DEGs in *D. alata* under different storage durations.**

## Differential expression of TFs in *D. alata* under different storage durations

A total of 1977 TFs were identified in *D. alata* samples under different storage durations. These TFs mainly belonged to ten families, including bHLH (122 genes), ERF (121 genes), MYB (111 genes), C2H2 (99 genes), NAC (98 genes), WRKY (97 genes), MYB-related (66 genes), FAR1 (78 genes), bZIP (75 genes), and GARP-G2-like. In addition, 666 TF genes were identified among the DEGs, and heatmaps of the top six TF families were generated (Fig. 8B). The expression patterns of TFs in these top six families were further analyzed as follows: Among the eight bHLH family genes, three mainly exhibited a down-regulation trend, while the other five showed a trend of first increasing and then decreasing. Specifically, four of these five genes reached their expression peak at 20 d, and one peaked at 10 d. Among the eight MYB family genes, one mainly showed a down-regulation trend, and the remaining seven displayed a trend of first increasing and then decreasing. Among these seven genes, one peaked at 10 d, three peaked at

20 d, and another three peaked at 30 d. Among the six ERF family genes, one mainly exhibited an up-regulation trend, one peaked at 30 d, one showed a trend of first increasing and then decreasing, and the other three displayed a down-regulation trend. Among the three WRKY family genes, one mainly showed a down-regulation trend, while the other two exhibited a trend of first increasing and then decreasing. Among the three NAC family genes, one mainly displayed an up-regulation trend and peaked at 30 d, and the remaining two showed a down-regulation trend. All three C2H2 family genes exhibited a down-regulation trend.

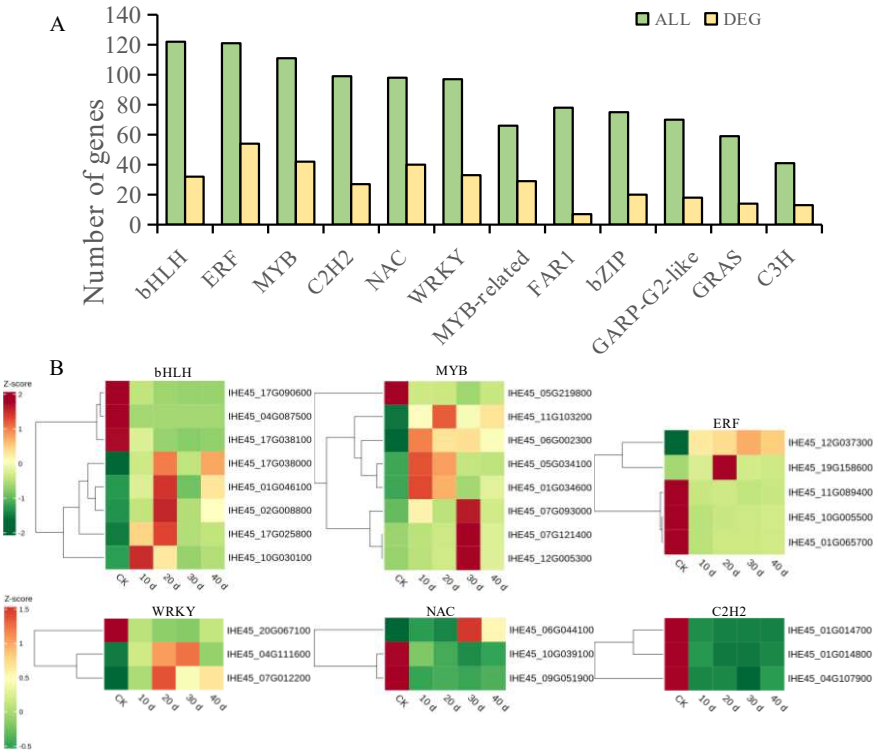


**Fig. 8. Number of TFs in *D. alata* with different storage time.** (A) Top TFs families according to gene number. (B) Heatmaps of TFs (bHLH, MYB, ERF, WRKY, NAC and C2H2) in the DEGs.

Furthermore, we systematically analyzed the dynamic expression profiles of 12 transcription factor genes during treatment using a combined qRT-PCR and RNA-Seq approach. The expression trends detected by the two techniques were highly consistent overall, which fully validated the reliability of the transcriptomic sequencing data and laid a solid foundation for subsequent functional studies. Based on their expression patterns, these genes were classified into two core regulatory groups (Fig. 9). The first group, which was significantly up-regulated after treatment, included bHLH1, MYB1, WRKY1, and NAC1. These genes maintained low expression levels from the CK to 10 d, peaked at 20 – 30 d, and remained relatively high at 40 d, indicating that they play key regulatory roles during the middle and late stages of treatment and serve as core candidate factors in response to treatment-induced stress. The second group, which was highly expressed in CK and continuously down-regulated after treatment, comprised MYB2, ERF1, ERF2, WRKY2, NAC2, C2H21, and C2H22. These genes exhibited high expression at the CK stage, decreased rapidly after treatment and remained at low levels, with only C2H22 showing a slight rebound at 40 d. This implies that these genes are involved in basic growth and metabolic processes, and their down-regulation is closely associated with the treatment-induced transition of physiological state. Temporal analysis revealed that 20-30 d represented the core window during

which gene expression changed most dramatically: up-regulated genes reached their peak expression levels, while down-regulated genes declined to their lowest points. This further confirms that this period serves as a key regulatory node in the response of the material to treatment.In summary, this study identified bHLH1, MYB1, WRKY1, and NAC1 as core candidate regulatory genes involved in treatment response, and defined 20-30 d as the critical response stage. These findings provide an important foundation for further dissecting the molecular regulatory mechanisms underlying the response of the material to treatment stress.

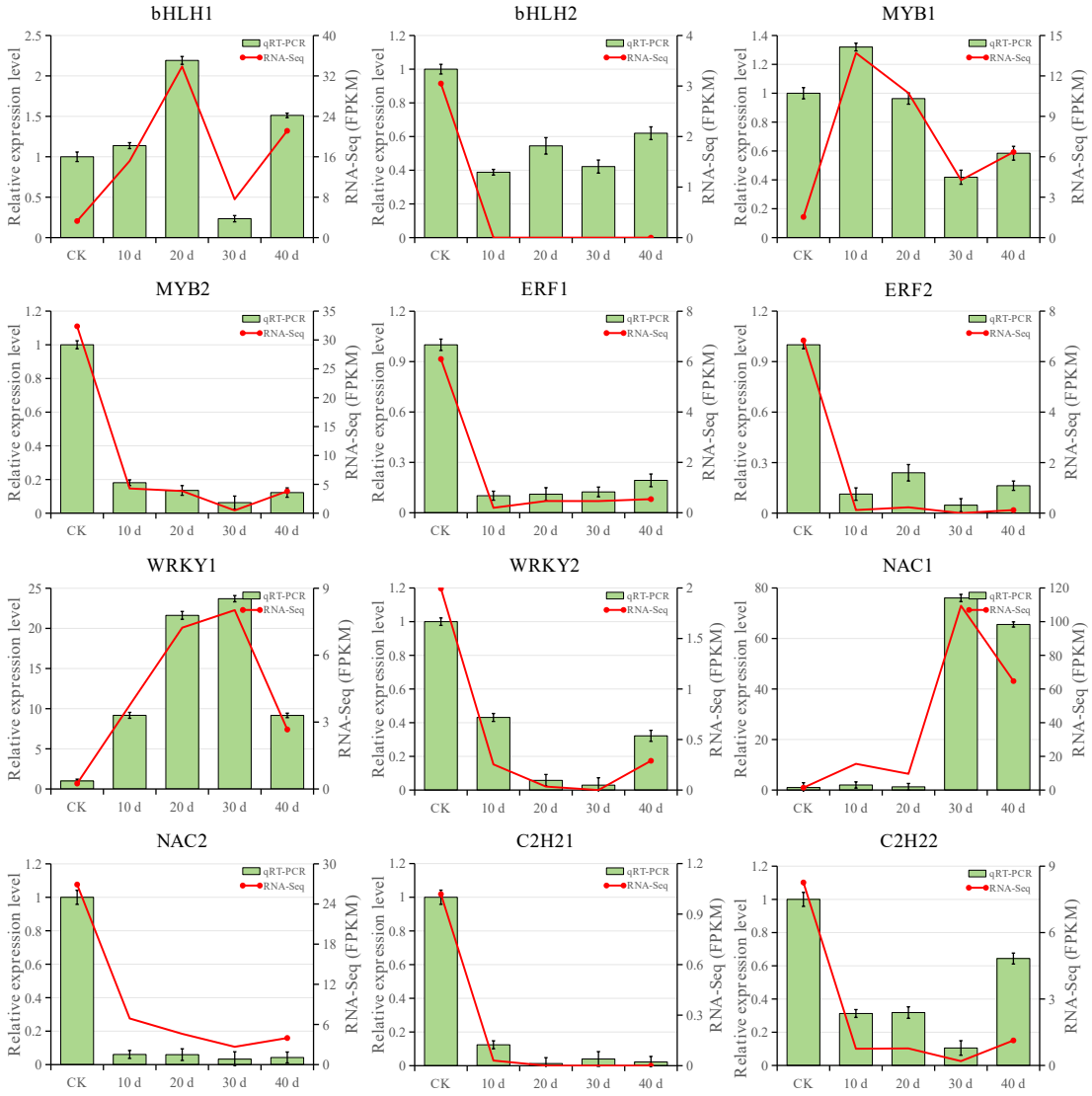


**Fig. 9. Expression patterns of 12 transcription factor genes at different treatment stages analyzed by qRT-PCR and RNA-Seq**. Green bars represent the relative expression levels determined by qRT-PCR (left Y-axis), and red lines with solid circles indicate the FPKM values from RNA-Seq (right Y-axis).

## Discussion

As a traditional Chinese medicinal and edible plant with the same origin of medicine and food, *D. alata* possesses irreplaceable nutritional and medicinal values. With the improvement of people's living standards, an increasing number of individuals have developed health-conscious behaviors such as healthy eating and health preservation, and have gradually recognized the clinical value of *D. alata*.

In this study, physiological indexes of *D. alata* planted in the scientific research base of Zhejiang Subtropical Crops Research Institute were systematically analyzed. The results showed that the water content decreased gradually during storage, which reflects the water loss of *D. alata* during the storage period. Total polysaccharide content decreased in the early storage stage (10–20 days), increased sharply around 30 days, and then decreased slightly after 40 days. Starch content showed a continuous downward trend, indicating that starch may undergo decomposition and other related reactions during the storage of *D. alata*. Amylopectin content decreased with the extension of storage time, which was consistent with the variation trend of total starch. VE content changed relatively gently in the early storage stage (10–20 days) and fluctuated or increased in the late stage (30–40 days). VC content remained low with little variation in the early stage (10–20 days), increased sharply around 30 days, and decreased again at 40 days. Amino acid content decreased first and then increased, with a significant increase observed after approximately 30 days of storage. Crude protein content first decreased and then increased significantly during the 30–40 day storage period. Crude fat content increased obviously in the late storage stage (30–40 days). In general, during the storage of *D. alata*, the contents of most nutrients (such as starch, protein, amino acids, and some vitamins) and water content decreased, while the content of reducing sugar increased due to starch transformation, leading to an overall decline in quality with prolonged storage (Fig. 1).

Correlation analysis results showed that starch content (including total starch and amylopectin) and water content both decreased with the extension of storage time. It is speculated that the reduction of water content may accelerate the decomposition of starch and other reactions, and there is a positive correlation between them (i.e., reduced water content facilitates starch decomposition and further decreases its content). Amino acids are the basic units of proteins, and crude protein content showed a similar “first decreasing and then increasing” trend to amino acid content, indicating a correlation between the two. During the process of protein decomposition and synthesis (or transformation), amino acids, as intermediates, showed a positive correlation trend with crude protein. As important vitamins, VE and VC exhibit antioxidant activities. When nutrients such as starch and protein decompose during storage, oxidative stress may occur, prompting VE and VC to exert their antioxidant functions. Therefore, there may be a negative correlation between the content changes of VE, VC and nutrient decomposition indexes (e.g., the decrease of starch content). However, the increase of some vitamins in the late storage stage may be related to substance transformation in *D. alata* (e.g., decomposition of polysaccharides into monosaccharides, which provide precursors for vitamin synthesis), and may be positively correlated with related substance transformation indexes. Crude fat content increased in the late storage stage, while the contents of carbohydrates such as starch decreased. It is speculated that there may be a transformation process from carbohydrates to fats, resulting in a negative correlation between crude fat content and starch content. Additionally, crude fat content may have a certain positive correlation with substances involved in this transformation (e.g., total polysaccharides, which first increased and then decreased in the late storage stage, with a partial overlap with the late-stage increase of crude fat) (Fig. 2).

DNBSEQ high-throughput sequencing is an effective method to obtain a large number of ESTs due to its high data volume and rich information. For species that have not yet been fully sequenced, high-throughput sequencing is an ideal approach to study the expression of important genes during growth and development, and has been widely applied in gene research of various

species. In this study, after filtering the original transcriptome sequences, 47.08 M, 45.91 M, 48.27 M, 53.78 M, and 46.49 M effective sequence reads were obtained from the five samples, respectively (Table 1). Compared with the published genome of *Dioscorea zingiberensis,* a wealth of genetic information was obtained in this study, which can be used for subsequent gene function analysis, gene cloning, and molecular marker development (Tamiru et al. 2017).

Statistical analysis of unigenes showed that 1688, 2548, 6945, and 2185 DEGs were identified in the 10 d vs CK, 20 d vs CK, 30 d vs CK, and 40 d vs CK groups, respectively, with 666 DEGs shared among the four groups. The numbers of up-regulated and down-regulated genes in the four groups both showed an upward trend, peaking at 30 d (Fig. 3). Functional characterization of DEGs based on GO and KEGG pathway enrichment analyses indicated that these genes or their encoded proteins are involved in cellular metabolism or carbon metabolism, and may play crucial regulatory roles in the storage of *D. alata* (Fig. 4).

K-means clustering results showed that all DEGs were classified into six distinct clusters, containing 2010, 488, 936, 781, 2729, and 1613 genes, respectively, with each cluster exhibiting distinct expression trends. Specifically, the C1 cluster showed a downward expression trend, the C2 cluster showed an initial upward trend followed by a downward trend, the C3 cluster increased in the first two stages and then decreased, the C4 cluster maintained a continuous upward trend throughout the entire storage period, the C5 cluster increased in the first three stages and then decreased, the C6 cluster decreased in the first three stages and then increased. From these results, it can be inferred that genes in the C2 cluster can be rapidly induced during storage, while genes in the C3, C4, and C5 clusters exhibit time-dependent expression trends during storage. Genes in the C1 and C6 clusters show an inhibitory expression trend during storage. In addition, KEGG pathway analysis of DEGs in the C4 and C5 clusters (up-regulated) and C1 and C6 clusters (down-regulated) showed that these DEGs are mainly related to metabolic pathways, biosynthesis of secondary metabolites, hormone signal transduction, and plant-pathogen interaction (Fig. 6), indicating that these pathways may play important regulatory roles in the storage of *D. alata*. GO annotation analysis showed that all selected DEGs were involved in 2677 pathways, especially the "molecular function" category, which contained a relatively large number of DEGs (Table 4). This indicates that *D. alata* maintains strong metabolic activity during storage.

Starch is the most important dietary energy source for humans, accounting for 80% of the total daily calorie intake, and thus plays a vital role in the food industry (Keeling et al. 2010; Bahaji et al. 2014; Tetlow et al. 2006). It is also a raw material for various industrial applications, with a global industrial demand of 180 million tons per year (Xu et al. 2017). Starch synthesis is synergistically catalyzed by various enzymes, such as UGP-glucose pyrophosphorylase (UGPaes), sucrose synthase (Susy), starch synthase (SS), ADP-glucopyranophosphatase (AGPase), and phosphoglucomutase (PMG) (Ahmed et al. 2018). The synthesis of starch is regulated by the expression of multiple enzyme-encoding genes (Deschamps et al. 2008). In this study, 14 DEGs involved in five metabolic pathways of starch and sucrose metabolism were identified (Fig. 7), including the metabolic processes of cellulose to cellodextrin, cellodextrin to cellobiose, starch/glycogen to dextrin, trehalose-6-phosphate to D-glucose-6-phosphate, and 1,3-β-glucan to D-glucose. These genes play important roles in starch and sucrose metabolism during the storage of *D. alata*.

TFs play vital regulatory roles in almost all biological processes, including plant growth and development, stress resistance, and pathogen defense (Zhang et al. 2011). It has been reported that

TFs can participate in the regulation of starch biosynthesis-related gene expression, thereby affecting starch quality and crop yield. For example, SUSIBA2, a member of the barley WRKY family, can directly bind to the sugar response element of iso1 and regulate its expression (Liu et al. 2015). Deletion and overexpression of the AP2/EREBP transcription factor RSR1 can affect amylopectin structure (Meng et al. 2020). SERF1 can directly bind to RPBF to regulate starch granule size and starch content (Schmidt et al. 2014). ZmDof3 is specifically expressed in maize endosperm, and its knockout can lead to the down-regulation of starch synthesis-related genes (Qi et al. 2017). ZmEREB94 can directly bind to the promoter of the *ZmSSI* gene and indirectly regulate the expression of ZmSh2 and ZmGBSSI, thereby participating in maize starch biosynthesis (Li et al. 2017). ZmMYB14 binds to the TAACTG element on the ZmBt1 promoter and participates in the transcriptional regulation of maize starch biosynthesis-related genes (Xiao et al. 2017). In this study, based on transcriptome data, a total of 1977 TFs were identified during the storage of *D. alata*, among which 633 TF genes were differentially expressed (DE-TFs). These DE-TFs mainly belonged to the bHLH, MYB, ERF, WRKY, NAC, and C2H2 gene families and exhibited distinct expression trends (Fig. 8). As one of the most important food crops worldwide, the molecular mechanism of starch biosynthesis-related genes in *D. alata* has been rarely reported compared with other crops. Studying TFs involved in starch synthesis in *D. alata* is helpful for analyzing the molecular regulatory pathways of starch biosynthesis-related enzyme gene expression, which is of great significance for improving the quality and yield of *D. alata* starch.

## Conclusion

In this study, physiological and transcriptomic analyses were conducted to reveal the differences in *D. alata* under different storage durations. Transcriptome sequencing was performed to annotate the obtained unigenes by comparing them with public databases, and it was found that 666 DEGs were shared across all four groups. K-means/phylogenetic clustering and GO functional annotation indicated that genes related to carbon metabolism might play a vital role in the storage of *D. alata*. In addition, the genes involved in starch and sucrose metabolism were analyzed in detail. Furthermore, TF genes from different families exhibited dynamic expression patterns, which may be crucial for the metabolism of *D. alata* during storage. Overall, *D. alata* has a wealth of functional genes. This study analyzed the distribution characteristics of these genes and clarified the distribution of metabolic pathways, providing transcriptomic support for quality analysis of *D. alata* and laying a foundation for subsequent research on its genomics, functional genes, and molecular markers.

**Funding information:** This work was supported by the project of "Sannong Jiufang" Agricultural Science and Technology Cooperation Program of Zhejiang Province (2024-2025): Research and Application of Prevention and Control Technologies for Continuous Cropping Obstacles of Authentic Root and Rhizome-based Medicinal Materials (2024SNJF035); Breeding of New Wheat and Potato Varieties (ZX2024001-4); Taishun County Innovation Center for Potato Elite Seed Breeding. Major Special Project of Agriculture (New Dry Grain Variety Breeding) of Zhejiang Province in the 14th Five-Year Plan Period (2021C02064-1-4).

**Author contributions:** Peilong Wang: Investigation; Methodology; Writing-original draft; Writing-review & editing. Li Guan: Writing-original draft; Writing-review & editing. Qiaoyi Zhang: Data curation; Formal analysis; Investigation. Xinyue Li: Formal analysis; Writing-review & editing. Jiaqi He: Investigation; Methodology. Wan Xu: Data curation; Formal analysis; Investigation. Zhimin Qiu: Investigation; Methodology. Gongkai Chen:

Writing-review & editing; Investigation; Funding acquisition; Methodology. Zhuang Zhou: Writing-review & editing, Supervision; Funding acquisition.

**Conflict of interest:** The authors declare that they have no known competing financial interests or personal relationships that could have appeared to influence the work reported in this paper.

**Data availability:** The data that support the findings of this study are available on request from the corresponding author.

## References


Ahmed S, Zhou X, Pang Y, Jin L and Bao JS (2018) Improving starch-related traits in potato crops: achievements and future challenges. *J. Starch - Starke*, 70, 9-10. doi: org/10.1002/star. 201700113.

Bahaji A, Li J, Sánchez-López AM, Baroja-Fernández E, Munoz FJ, Ovecka M, Almagro G, Montero M, Ezquer I, Etxeberria E and Pozueta-Romero Ovecka J (2014) Starch biosynthesis, its regulation and biotechnological approaches to improve crop yields. *J. Biotechnology Advances*, 32, 87-106. doi: 10.1016/j.biotechadv.2013.06.006.

Chen K, Fan DY, Fu B, Zhou JZ and Li HR (2018) Comparison of physical and chemical composition of three chinese jujube (*Ziziphus Jujuba* Mill.) cultivars cultivated in four districts of xinjiang region in China. *J. Food Science and Technology*, 2061, 1-10. doi: 10.1590/fst.11118.

Conesa A, Gotz S, Garcia-Gomez JM, Terol J, Talon M and Robles M (2005) Blast2go: a universal tool for annotation, visualization and analysis in functional genomics research. *J. Bioinformatics*, 21(18), 3674-3676. doi: 10.1093/bioinformatics/bti610.

Deng HN, Ru J, Liang Z, Tang Z, Wang Y, Yuan W, Li L, Feng Y and Gao X (2026) Single-cell transcriptomics reveals cellular and genetic mechanisms of alpine adaptation in *Rosa sericea*. *J. Front. Plant Sci*, 17, 1733247. doi: 10.3389/fpls.2026.1733247.

Deschamps P, Haferkamp I, Hulst CD, Neuhaus HE and Ball SG (2008) The relocation of starch metabolism to chloroplasts: when, why and how. *J. Trends in Plant Science*, 13, 574-582. doi: 10.1016/j.tplants.2008.08.009.

Ernst J and Bar-Joseph Z (2006) STEM: a tool for the analysis of short time series gene expression data. *J. BMC Bioinformatics*, 7(191), 1-11. doi: 10.1186/1471-2105-7-191.

Fang P, Niu SH, Yuan HW, Li ZX, Zhang YC, Yuan L and Li W (2014) Development and characterization of 25 EST-SSR markers in *Pinus sylvestris* var.*mongolica* (Pinaceae). *J. Applications in Plant Sciences*, 2(1), 1300057. doi: 10.3732/apps.1300057.

Feng YH, Yang ZQ, Wang J, Luo QF and Li HG (2014) Development and characterization of SSR markers from *Pinus massoniana* and their transfer ability to *P.elliottii, P.caribaea* and *P.yun-nanensis*. *J. Genetics & Molecular Research*, 13(1), 1508-1513. doi: 10.4238/2014.March.12.2.

Gao J, Tang YM, Luo FY, Tian YX and Luo JH (2022) Quality changes of fresh-cut yams under different shelf-life temperatures. *J. Food and Fermentation Industries*, 48(6), 98-102. doi: 10.13995/j.cnki.11-1802/ts.027576.

GB 5009.6-2025. National Food Safety Standard - Determination of fat in foods. Beijing: Standards Press of China. 2025.

Gebeyehu A, Hammenhag C, Tesfaye K, Vetukuri RR, Ortiz R and Geleta M (2026) Transcriptome analysis identifies genes regulating self-compatibility, flowering time, and oil biosynthesis in Noug (*Guizotia abyssinica*). *J. Scientific Reports*, 15(1), 1-19. doi: 10.1038/s41598-025-18728-x.

Grabherr MG, Haas BJ, Yassour M, Levin JZ, Thompson DA, Amit I, Adiconis X, Fan L, Raychowdhury L and Zeng Q (2011) Full-length transcriptome assembly from RNA-Seq data without a reference genome. *J. Nat.*

*Biotechnol*, 29, 644-652. doi: 10.1038/nbt.1883.

Gu L, Lu ML, Jiang J and Zhou XL (2006) Study on the polyphenol oxidase enzymology and anti-browning effects of yam. *J. Food & Machinery*, 22(6), 26-29. doi: 10.13652/j.issn.1003-5788.2006.06.008.

Gündüz GT and Korkmaz A (2019) UV-C treatment for the inhibition of molds isolated from dried persimmons (*Diospyros kaki* L.) and modelling of UV -C inactivation kinetics. *J. LWT-Food of Science and Technology*, 115, 10845-10857. doi: 10.1016/j.lwt.2019.108451.

He Z, Zeng J, Hu J, Chen J, Peng D, Du B and Pan L (2024) Effects of cooking methods on the physical properties and in vitro digestibility of starch isolated from Chinese yam. *J. International Journal of Biological Macromolecules*, 2, 131597-131603. doi: 10.1016/j.ijbiomac.2024.131597.

Jiang JX and Zhang TZ (2003) Extraction of total RNA in cotton tissues with ctab-acidic phenolic method. *J. Acta Gossypii Sin*, 15, 166-167. doi: 1002-7807（2003）03-0166-02.

Jing X, Jiang H, Du HH and Meng YF (2016) Research Progress on *Dioscorea opposita* in China. *J. Journal of Anhui Agri Sc*, 44(15), 114-117. doi: 10.3969/j.issn.0517-6611.2016.15.040.

Minoru K, Susumu G, Shuichi K, Yasushi O and Masahiro H (2004) The KEGG resource for deciphering the genome. *J. Nucleic Acids Research*, 32(22), 277-280. doi: 10.1093/nar/gkh063.

Keeling PL and Myers AM (2010) Biochemistry and genetics of starch synthesis. *J. Annu Rev Food Sci Technol*, 1, 271-303. doi: 10.1146/annurev.food.102308.124214.

Kim TE, Lee JH, Kim YJ, Lee MH, Jang HW, Chun YG and Kim BK (2025) Simultaneous quantitation and stability evaluation of cholecalciferol and α-Tocopherol in vitamin-fortified nanoemulsions by UHPLC–MS/MS coupled with QuEChERS extraction. *J. ACS Food Science & Technology*, 5(1), 112–121. doi: 10.1021/acsfoodscitech.4c00841.

Li D, Yang SA, Zhang XZ, Qin MX and Guan JF (2024) Effects of different concentration edible alcohol on browning and texture quality of fresh-cut yams during storage. *J. Food Science and Technology*, 49(02), 32-39. doi: 10.13684/j.cnki.spkj.2024.02.006.

Li H, Xiao QL, Zhang CX, Du J, Li X, Huang HH, Wei B, Li YP, Yu GW, Liu HM, Hu YF, Liu YH, Zhang JJ and Huang YB (2017) Identification and characterization of transcription factor ZmEREB94 involved in starch synthesis in maize. *J. Journal of Plant Physiology*, 216, 11-16. doi: 10.1016/j.jplph.2017.04.016.

Li X, Bao ZY, Chen YN, Lan Q, Song C, Shi L, Chen W, Cao S, Yang Z and Zheng Q (2023) Exogenous glutathione modulates redox homeostasis in okra (*Abelmoschus esculentus*) during storage. *J. Postharvest Biology and Technology*, 195(1), 112145. doi: 10.1016/j.postharvbio.2022.112145.

Li Y, Ji SY, Xu T, Zhong YH, Xu MH, Liu YQ, Li MJ, Fan B, Wang FZ, Xiao JB and Lu BY (2023) Chinese yam (*Dioscorea*): Nutritional value, beneficial effects, and food and pharmaceutical applications. *J. Trends in Food Science & Technology*, 134, 29-40. doi: org/10.1016/j.tifs.2023.01.021.

Liao J, Liao WX and Wang BL (2021) Effect of fresh cutting and steaming on store quality of glutionous yam. *J. Bulletin of Fermentation Science and Technology*, 50(2), 63-69. doi: 10.16774/j.cnki.issn.1674-2214.2021.02.001.

Liu HL, Li J, Wang QZ, Liu JH, Feng XT and Yan SL (2015) Study on the Chinese fresh-cut yam preserved by high concentration of ethanol solution. *J. Journal of Food Safety and Quality*, 6(07), 2509-2515. doi: 10.19812/j.cnki.jfsq11-5956/ts.2015.07.024.

Ma LH, Qin WD, Chen XH and Wang L (2012) Effect of coating on browning and antioxidant activity of fresh-cut yam. *J. Food Science*, 33(18), 6. doi: 1002-6630(2012)18-0275-06.

Ma ZY, Yu XX, Yang SQ and Yuan Q (2021) Effect of ice temperature storage technology on quality of fresh- cut yam and shelf life prediction. *J. Farm Products Processing*, 2, 4-9. doi: 10.16693/j.cnki.1671-9646(X).2021.01.036.

Meng Y, Wang TT, Zhang F, Chen DJ and Zhang YH (2020) Effects of different treatments on the quality of fresh-cut yam. *J. J. Anhui Agric. Sci*, 48(07), 198-201. doi: 10.3969/j.issn.0517-6611.2020.07.057.

Phosarith N, Siriwoharn T and Jirarattanarangsri W (2025) Comparison of the conventional, chemical, and ultrasound extraction of crude polysaccharides and their properties from *Lentinula edodes* (*Berk.*) *Pegler*. *Foods*, 14(14), 2428. doi: 10.3390/foods14142428.

Qi X, Li SX, Zhu YX, Zhao Q, Zhu DY and Yu JJ (2017) *ZmDof3*, a maize endosperm-specific Dof protein gene, regulates starch accumulation and aleurone development in maize endosperm. *J. Plant Molecular Biology*, 93(1), 7-20. doi: 10.1007/s11103-016-0543-y.

Rajkumar AP, Qvist P, Lazarus R, Lescai F, Ju J, Nyegaard M, Mors O, Børglum AD, Li QB and Christensen JH (2015) Experimental validation of methods for differential gene expression analysis and sample pooling in RNA-seq. *J. BMC Genomics*, 16, 548-556. doi: 10.1186/s12864-015-1767-y.

Schmidt R, Schippers JHM, Mieulet D, Watanabe M, Hoefgen R, Guiderdoni E and Mueller-Roeber B (2014) SALT-RESPONSIVE ERF1 is a negative regulator of grain filling and gibberellin-mediated seedling establishment in rice. *J. Molecular Plant*, 7(2), 404-421. doi: 10.1093/mp/sst131.

Tamiru M, Natsume S, Takagi H, White B,Yaegashi H, Shimizu M, Yoshida K, Uemura A, Oikawa K and Abe A (2017) Genome sequencing of the staple food crop white Guinea yam enables the development of a molecular marker for sex determination. *J. BMC Biology*, 15, 1-20. doi: 10.1186/s12915-017-0419-x.

Tang H, Feng GY, Deng ML, Ouyang Q, Liu XJ, Jiang XJ, Tian MZ, Yang G, Xiang Q and Li R (2026) Digestible indispensable amino acid score of energy-providing ingredients commonly used in diets. *British Journal of Nutrition*, 1–12. doi: 10.1017/S0007114525106016.

Tatusov RL, Galperln MY, Natale DA and Koonin EV (2000) The COG database: A tool for genome-scale analysis of protein functions and evolution. *J. Nucleic Acids Research*, 28(1), 33-36. doi: 10.1093/nar/28.1.33.

Tetlow IJ (2006) Understanding storage starch biosynthesis in plants: a means to quality improvement. *J. Canadian Journal of Botany*, 84, 1167-1185. doi: 10.1139/b06-089.

Wang M, Xu L, Wang MF and Tang J (2017) Effect of compound preservative on fresh-keeping of fresh-cut yam. *J. Food & Machinery*, 33(05), 134-140. doi: 10.13652/j.issn.1003-5788.2017.05.028.

Wassie KB (2025) Nutrient composition and antinutritional evaluation of selected wild edible plants grown in agroforestry of simada district, ethiopia. *The Scientific World Journal*, 1-8. doi: 10.1155/tswj/3545895.

Wu WY, Sun JJ, Han YW, Tang JQ and Jiang BL (2025) Research on the influence of different processing methods on the quality of 3 kinds of yam. *J. Agricultural Products Processing*, 12, 27-31. doi: 10.16693/j.cnki.1671-9646(X).2025.12.006.

Xiao QL, Wang YY, Du J, Li H, Wei B, Wang Y, Li Y, Yu G, Liu H and Zhang J (2017) *ZmMYB14* is an important transcription factor involved in the regulation of the activity of the *ZmBT1* promoter in starch biosynthesis in maize. *J. Febs Journal*, 284(18), 3079-3099. doi: 10.1111/febs.14179.

Xu X, Dees D, Dechesne A, Huang XF and Trindade LM (2017) Starch phosphorylation plays an important role in starch biosynthesis. *J. Carbohydrate polymers*, 157, 1628-1637. doi: 10.1016/j.carbpol.2016.11.043.

Yang FX, Wang JX, Zhu H and Si WF (2018) Antibacterial pretreatment and fresh-keeping packaging of fresh cut yam. *J. Packaging Journal*, 10(2), 6. doi: 10.3969/j.issn.1674-7100.2018.02.010.

Ye J, Fang L, Zheng HK, Zhang Y, Chen J, Zhang ZJ, Wang J, Li ST, Li RQ, Bolund L and Wang J (2006) WEGO: a web tool for plotting go annotations. *J. Nucleic Acids Res*, 34, 293-297. doi: 10.1093/nar/gky400.

Zhang JY, Qu SC, Guo ZR, Du XL, Du BB and Zhang Z (2011) Biology function of bZIP transcription factors in plants. *J. Acta Bot Boreal. -Occident. Sin*, 31(5), 1066-1075. doi: 10.1631/jzus.B1000171.

Zheng JH, Yang L, Ma W, Yin HX, Fu WJ and Zhang XY (2026) Transcriptome analysis and functional validation of JAZ subfamily genes of *Sesuvium portulacastrum* under salt and cadmium stresses. *J. Int. J. Mol. Sci*, 27,

2101. doi: 10.3390/ijms27052101.

Zheng Y, Jiao C, Sun HH, Heman GR, Marina AP, Zhang PF and Michael B (2016) iTAK: A program for genome-wide prediction and classification of plant transcription factors, transcriptional regulators, and protein kinases. *J. Molecular Plant*, 9, 1667-1670. doi: 10.1016/j.molp.2016.09.014.